Classical theory of laser-assisted spontaneous bremsstrahlung

H. B Ambalampitiya and I. I. Fabrikant

Department of Physics and Astronomy,

University of Nebraska, Lincoln, Nebraska 68588-0299, USA

(Dated: May 3, 2019)

Abstract

We study the process of laser-assisted spontaneous electron bremsstrahlung by running classical trajectories in a combined Coulomb and laser (ac) fields. Due to chaotic scattering in the combined Coulomb and ac fields, the radiation probability as a function of the impact parameter and the constant phase of the laser field exhibits fractal structures. However, these structures are smeared out when the cross section is integrated over the impact parameter and averaged over the phase. We analyze the role of different types of orbits, including the trapped orbits, and the dependence of the radiation probability on the impact parameter and the initial phase of the ac field. We show for the first time that at low incident electron kinetic energy the Coulomb focusing leads to a substantial extension of the range of impact parameters contributing to the bremsstrahlung cross section and results in a substantial increase (by one to two orders of magnitude) of the cross section as compared to the pure Coulomb case. As examples, we discuss the case of relatively high ponderomotive energy E_p when we obtain an efficient production of photons with frequencies up to $2E_p$, and the case of low E_p when only infrared photons are produced. Overall accuracy of the classical approach is estimated as very good, although it does not describe resonant processes studied previously by quantum-mechanical methods.

PACS numbers:

I. INTRODUCTION

Laser-assisted spontaneous bremsstrahlung is a process of creation of a photon with frequency Ω due to electron-atom scattering in the presence of an ac field of a lower frequency ω, i.e. the process

$$n\hbar\omega + e + A \to n'\hbar\omega + \hbar\Omega + e + A.$$

It is different from the stimulated bremsstrahlung when the emitted photon has the same frequency as the initial photon. Laser-assisted spontaneous bremsstrahlung is in fact the same as the harmonic generation in the continuum. We will be interested in the process when the atomic system A is a bare nucleus or a positive ion, then the bremsstrahlung process is more efficient. Accordingly, we will model $e - A$ interaction by the Coulomb potential

$$V(r) = -\frac{Ze^2}{r}$$

where Z is the charge of the positive ion.

This process has been studied since 1970s [1–6]. More recent research [7–15] was stimulated by development of intense lasers. Most of these papers, particularly those dealing with relativistic electrons, were treating the electron-ion interaction in the first order of perturbation theory. Some exceptions [8, 9, 12, 16] were concentrating on the resonance processes when the frequency of the emitted photon equals an integer times the laser frequency. A more recent paper [17] analyzed the plateau structure due to rescattering similar to that in high-order harmonic generation.

Here we investigate another feature of the process relevant to low-energy electron scattering when the Coulomb interaction cannot be treated perturbatively. It is known that the laser-induced atomic ionization processes can be enhanced by the Coulomb focusing [18–25]. The action of the Coulomb potential, in combination with multiple electron returns due to the laser field, focuses parts of the electron wave function, increasing the efficiency of such processes as multiphoton ionization. Similar effects can occur in continuum-continuum transitions which are the subject of studies of the present paper.

In contrast to the ionization problem, the bremsstrahlung problem can be treated purely classically as long as the electron kinetic energy is small compared to its potential energy at the distances equal to the electron de Broglie wavelength [26] (sec. 49). This leads to the condition $\nu \gg 1$ where ν is the Coulomb parameter $\nu = Ze^2/(\hbar v)$ (v is the electron

velocity). This condition should be modified in the presence of an ac laser field as discussed below. It will be also shown that the range of validity of the classical approach is even broader than suggested by the condition $\nu \gg 1$. Some discrepancies between classical and quantum results for the laser-assisted bremsstrahlung problem were discussed in [7] and were shown to be not due to the failure of classical mechanics but due to the difference in description of electron states (localized wave packet versus the Volkov wave). It should be also added that, according to the Heisenberg correspondence principle, the quantum-mechanical matrix element of the electron dipole moment can be replaced by the Fourier transform of the corresponding classical quantity which leads to the classical result for the effective cross section for the spontaneous bremsstrahlung.

Classical treatment of electron motion in a combined Coulomb and ac fields was given by Wiesenfeld [27, 28]. He found that in a certain range of initial parameters this motion becomes chaotic and exhibits a fractal structure when a final parameter, like the deflection angle, is plotted as a function of the (initial) impact parameter. The irregular behavior is associated sometimes with the electron capture in an unstable bound orbits. This kind of behavior was studied by Leopold and Percival [29] in connection with the classical ionization problem in a microwave field. From the quantum-mechanical point of view, the electron is captured into a Rydberg orbital, and then performs a diffusion through a manifold of Rydberg states. The correspondence between classical chaotic behavior and quantum mechanics was addressed in the past (see, for example Ref. [30, 31]). In the present paper we will concentrate on the classical aspects of the problem. In particular, for the first time we analyze in detail the dependence of the radiation probability on the impact parameter and the initial phase of the ac field.

II. BASIC EQUATIONS

Consider electron beam moving in an external field. For a given trajectory the energy of radiation emitted in the frequency interval $d\Omega$ is ([32], Eq. (67.10))

$$dE_\Omega = \frac{2e^2}{3\pi c^3}|\ddot{\mathbf{r}}_\Omega|^2 d\Omega = \frac{2e^2\Omega^4}{3\pi c^3}|\mathbf{r}_\Omega|^2 d\Omega$$

where $\mathbf{r}_\Omega$ is the Fourier transform of the electron trajectory for a given impact parameter b

$$\mathbf{r}_\Omega(b) = \int_{-\infty}^{\infty} e^{i\Omega t}\mathbf{r}(b,t)dt \tag{1}$$

The total effective radiation (energy times cross section) per unit frequency in the case of cylindrical symmetry is given by

$$\frac{d\kappa_\Omega}{d\Omega} = 2\pi \int_0^\infty \frac{dE_\Omega}{d\Omega} b db. \tag{2}$$

In what follows we will be presenting the probability of a photon emission per unit frequency

$$P(b,\Omega) = \frac{1}{\hbar\Omega}\frac{dE_\Omega}{d\Omega} \tag{3}$$

and the cross section for emitting one photon per unit frequency

$$S(\Omega) = \frac{1}{\hbar\Omega}\frac{d\kappa_\Omega}{d\Omega} \tag{4}$$

In the case of the laser-assisted bremsstrahlung we are interested in the following potential

$$V(r) = -\frac{Ze^2}{r} - F_0 z\cos(\omega t + \varphi_0) \tag{5}$$

where the first term is due to the Coulomb field of the nucleus, and the second due to the external laser field with the linear polarization along the z axis. Generally the incident beam makes some angle with the z axis, but in the present paper we limit ourselves by the case when the incident velocity is parallel to the polarization of the laser field. Then the cylindrical symmetry of the problem is preserved, the conserved z component of angular momentum is 0, and the motion is planar. Fig. 1 presents a schematic view of a classical trajectory of an electron which is undergoing spontaneous bremsstrahlung in the potential given by Eq. (5)

We will concentrate on the case when the electron initially has a relatively low velocity of about 0.1 a.u. at the distance from the center of few hundred Bohr. Then, depending on the initial phase φ_0, field strength F_0 and ac field frequency ω, the electron can get close to the Coulomb center, or be reflected from the interaction region. In the former case the radiation will be efficient, in the latter, it is negligible. If the ponderomotive energy

$$E_p = \frac{F_0^2}{4m\omega^2}$$

equals a few a.u. the electron speed in the interaction region at the distance of a few Bohr from the Coulomb center, can reach 2-3 a.u. Therefore we will discuss first major features of bremsstrahlung in this velocity range. Since these velocities are small compared to the speed of light, $c = 137$ a.u., relativistic effects can be safely neglected.

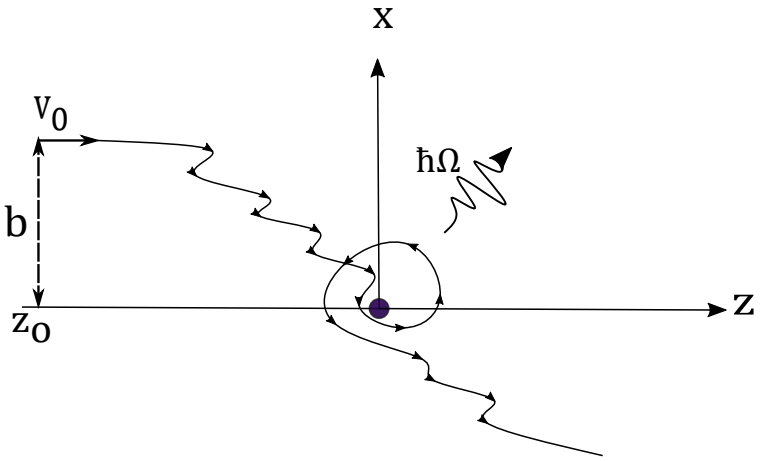

FIG. 1: A schematic for a classical trajectory of an electron undergoing spontaneous bremsstrahlung. The electron radiates a photon with frequency Ω as it is being accelerated by the Coulomb and laser fields.

III. BREMSSTRAHLUNG IN THE COULOMB FIELD

A. Comparison of classical and quantum approaches

In case $F_0 = 0$ the analytical solution is known in both classical and quantum theories. From now on we will use atomic units and assume that the nucleus is infinitely heavy. Then in the classical theory, ([32], Eq. (70,18))

$$P(b,\Omega) = \frac{\pi Z^2 \Omega}{6c^3 E^2}\left\{\left[H_{i\mu}^{(1)'}(i\mu\epsilon)\right]^2 - \frac{\epsilon^2-1}{\epsilon^2}\left[H_{i\mu}^{(1)}(i\mu\epsilon)\right]^2\right\} \tag{6}$$

where $E = v_0^2/2$ is the initial electron kinetic energy, $\mu = Z\Omega/v_0^3$, and ϵ is the eccentricity of the hyperbolic orbit

$$\epsilon^2 = 1 + \frac{v_0^4 b^2}{Z^2},$$

$H_p^{(1)}(x)$ is the Hankel's function, and prime means the derivative with respect to its argument.

The total cross section per unit frequency ([32], Eq. (70,19)) is

$$S(\Omega) = \frac{4\pi^2 Z^3}{3c^3 v_0^5}|H_{i\mu}^{(1)}(i\mu)|H_{i\mu}^{(1)'}(i\mu). \tag{7}$$

For calculations it is convenient to express the Hankel function and its derivative through the real modified Bessel function of the third kind $K_{i\mu}(x)$

$$H_{i\mu}^{(1)}(i\mu\epsilon) = \frac{2}{\pi i}e^{\pi\mu/2}K_{i\mu}(\mu\epsilon)$$

$$H_{i\mu}^{(1)'}(i\mu\epsilon) = -\frac{2}{\pi} e^{\pi\mu/2} K'_{i\mu}(\mu\epsilon)$$

At large μ corresponding to large frequencies calculation of $K_{i\mu}(\mu\epsilon)$ by either power series or asymptotic series becomes impossible, and we use uniform Airy function approximation discussed in Appendix A.

The quantum cross section is given by the equation ([33], Eq. (92,15))

$$S(\Omega) = \frac{64\pi^2 Z^2}{3c^3\Omega} \frac{v}{v_0(v_0 - v)^2} \frac{1}{(1 - e^{-2\pi\nu})(e^{2\pi\nu_0} - 1)} \left(-\frac{d}{d\xi} |F(\xi)|^2 \right)$$

where v is determined from the conservation of energy

$$v_0^2 = v^2 + 2\Omega,$$

ν_0 and ν are the Coulomb parameters for the initial and final state, $\nu_0 = Z/v_0$, $\nu = Z/v$, and $F(\xi)$ is the hypergeometric function

$$F(\xi) = F(i\nu, i\nu_0, 1, \xi), \quad \xi = -\frac{4v_0 v}{(v_0 - v)^2}.$$

As apparent from the above equations, the important deficiency of the classical treatment is in the neglect of the electron energy loss due to radiation. This should become a concern when the electron incident energy $E_0 = v_0^2/2$ is comparable to the energy $\hbar\Omega$ of the radiated photon. Moreover, it seems first that for $\Omega > E_0/\hbar$ radiation is simply not possible, and for small incident electron velocities of about 0.1 a.u. the range of Ω is limited to infrared and microwaves. However, two important points relax these restrictions. First, the quantum bremsstrahlung does not really have the well-defined high-frequency cut-off because of the possibility of the further loss of electron energy due to capture into Rydberg states [33]. Indeed, the quantum cross section is finite at $\Omega = E_0/\hbar$. In Fig. 2 we present comparison of classical and quantum bremsstrahlung cross sections in the Coulomb field for two electron velocities. Although at $v_0 = 2$ a.u. the formal cut-off frequency is $\Omega = 2$ a.u., the quantum cross section remains finite at this frequency. Moreover, we see that classical and quantum cross sections agree very well even for velocities corresponding to a relatively low Coulomb parameter $\nu_0 = Z/v_0$. (The classical limit corresponds to large ν_0).

Second, and more important, when the ac field is added, the electron, when approaching the Coulomb center, might have the kinetic energy which is much higher than its initial kinetic energy if the ponderomotive energy E_p is high. In what follows we choose an illustrative case with ponderomotive energy about 3 a.u. In case of a favorable phase φ_0, the

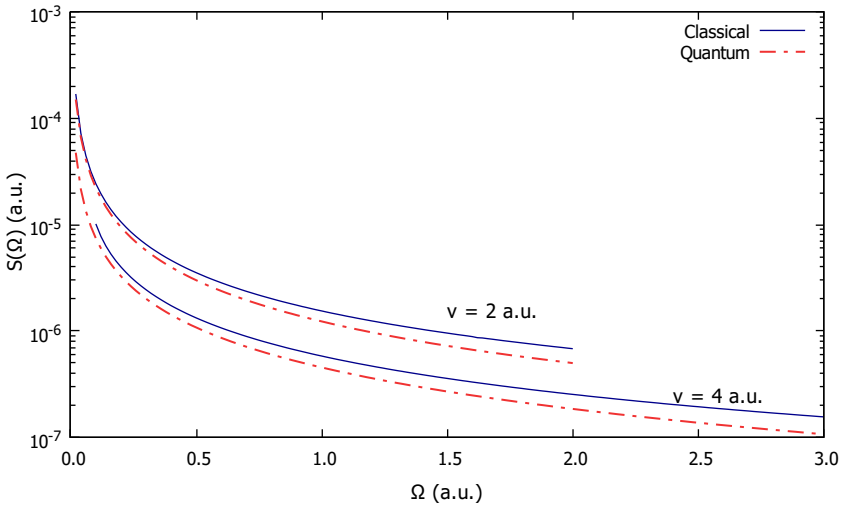

FIG. 2: The bremsstrahlung cross section in the Coulomb field (Z=1) without the ac field for two electron velocities. For each velocity the solid (blue) curve represents the classical result, and the dash-dotted (red) curve, the quantum result.

electron kinetic energy at a distance of a few a.u. from the Coulomb center typically reaches $2E_p$, corresponding to velocity of about 3.5 a.u. For this velocity the classical treatment, as follows from Fig. 2, is reasonably accurate. Second, at this velocity electron is allowed to emit photons with energies of up to about 6 a.u. Although the classical theory does not produce the rigorous cut-off frequency, it will be safe to assume that electron can emit photons with energies up to 3 a.u.

We conclude that even for small incident velocities the bremsstrahlung process can generate high-frequency UV radiation in case of favorable initial conditions and high enough ponderomotive energy, and the quantum effects play a minor role in this case. This agrees with the remarkable classical-quantum correspondence for the motion in the Coulomb potential. In particularly the Rutherford scattering cross section is the same in both theories.

B. Calculation of electron trajectories in the Coulomb field

The accuracy of numerical methods for calculation of classical trajectories can be verified in the case $F_0 = 0$. Consider the Coulomb scattering in the zx plane. The equations for a hyperbolic trajectory are

$$z = a(\epsilon - \cosh\xi), \qquad x = b\sinh\xi, \qquad t = \frac{a}{v_0}(\epsilon\sinh\xi - \xi)$$

where $a = Ze^2/v_0^2$ is the semimajor axis, and we use $a(\epsilon^2 - 1)^{1/2} = b$.

At $t \to -\infty$ the trajectory approaches asymptotically the straight line which makes angle α with the z axis defined as

$$\tan\alpha = \frac{b}{a}.$$

In numerical calculations the velocity of the incident electron is parallel to the z axis. Therefore we perform the rotation by the angle α.

$$z' = z\cos\alpha + x\sin\alpha, \qquad x' = -z\sin\alpha + x\cos\alpha$$

or

$$z' = \frac{1}{\epsilon}\left(z + \frac{b}{a}x\right), \qquad x' = \frac{1}{\epsilon}\left(-\frac{b}{a}z + x\right)$$

so that at $t \to -\infty$ $z' \to -\infty$, $x' \to -b$.

Above equations can be compared with numerical calculations. The results of applications of numerical algorithms of the Runge-Kutta type exhibit strong instabilities due to the Coulomb singularities. It is well known that instabilities occur because these methods generally do not conserve energy and do not satisfy the canonical transformation requirement. Although this problem can be resolved by using the symplectic algorithms [34, 35], we found the method based on the extended Hamiltonian and canonical transformation of the time coordinate is more efficient for hyperbolic trajectories, see Appendix B.

To avoid numerical difficulties, many classical and quantum calculations of strong-field ionization and high-order harmonic generation use the soft-Coulomb potential [36–38] which is finite at the origin. We stress that in the bremsstrahlung problem the full account of the Coulomb interaction, including the short distances, is necessary, since the most of radiation occurs at small distances.

IV. BREMSSTRAHLUNG IN THE AC FIELD

For calculation of Fourier transform of Cartesian components of acceleration, we use alternately acceleration, velocity, and the length form, depending on the distance from the Coulomb center. Details are presented in Appendix C.

In Fig. 3 we present $P(b, \Omega)$ with addition of the ac field with parameters $F_0 = 0.05338$ a.u. (intensity $I = 100$ TW/cm^2), $\omega = 0.0147$ a.u. (wavelength $\lambda = 3.1$ μm), $\varphi_0 = 0$. Integration always starts with $z_0 = -300$ a.u. where the Coulomb field can be safely neglected.

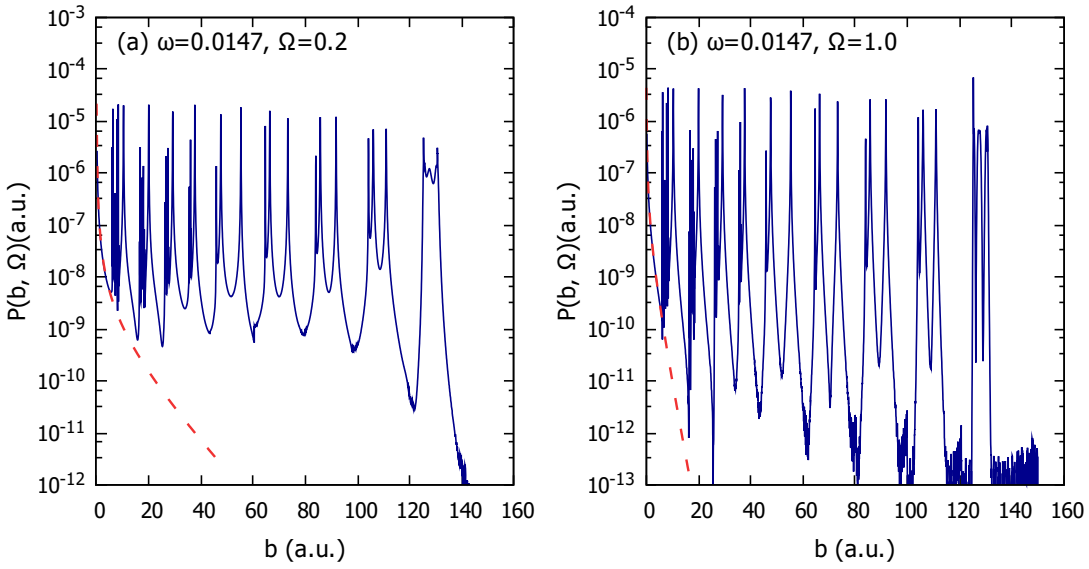

FIG. 3: (a) $P(b,\Omega)$ as a function of the impact parameter b for the case, $Z = 1$, $v_0 = 0.1$ a.u. $F_0 = 0.05338$ a.u., $\omega = 0.0147$ a.u., and $\Omega = 0.2$ a.u. Red dashed curve: pure Coulomb case for $v_0 = 3.56$ a.u.. (b) The same as in panel (a) except $\Omega = 1.0$ a.u.

In this situation averaging of results over z_0 is equivalent to averaging over the phase φ_0 [7]. To compare this probability with the probability of the field-free bremsstrahlung, we have chosen the electron velocity $v = 3.56$ a.u. (kinetic energy 6.35 a.u.) corresponding to a typical velocity of electron in the ac field with the ponderomotive energy $E_p = F_0^2/4\omega^2 = 3.30$ a.u.

Two striking differences with the pure Coulomb case are immediately noticeable. First, in the laser-assisted case $P(b,\Omega)$ exhibits very sharp quasiperiodic structures. By expanding the b scale, as shown in Fig. 4, we can see that the structure is a fractal as was observed before for the deflection angle as a function of the impact parameter b [27, 28] for b below the quivering length $l = F_0/\omega^2$. This fractal structure is caused by chaotic scattering which was demonstrated by investigation of deflection angle as a function of b for several stationary problems [39–41]. In our case $l = 247$ a.u., therefore the condition $b < l$ [27] is satisfied in the whole range of b where $P(b,\Omega)$ is non-negligible.

Second, the range of impact parameters b contributing to the total cross section is much larger than in the pure Coulomb case. Both features can be explained by the behavior of trajectories in the combined laser and Coulomb fields.

In Fig. 5 we present two trajectories for impact parameter $b = 47.60$ and 51.55 a.u. The

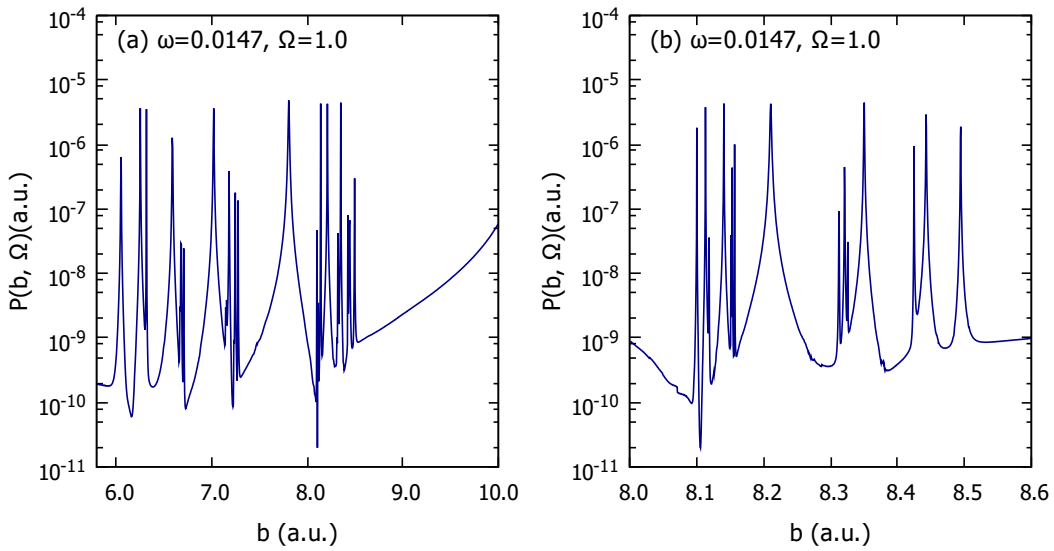

FIG. 4: (a) The same as in Fig. 3b but on an expanded b scale. (b) The b scale is expanded further.

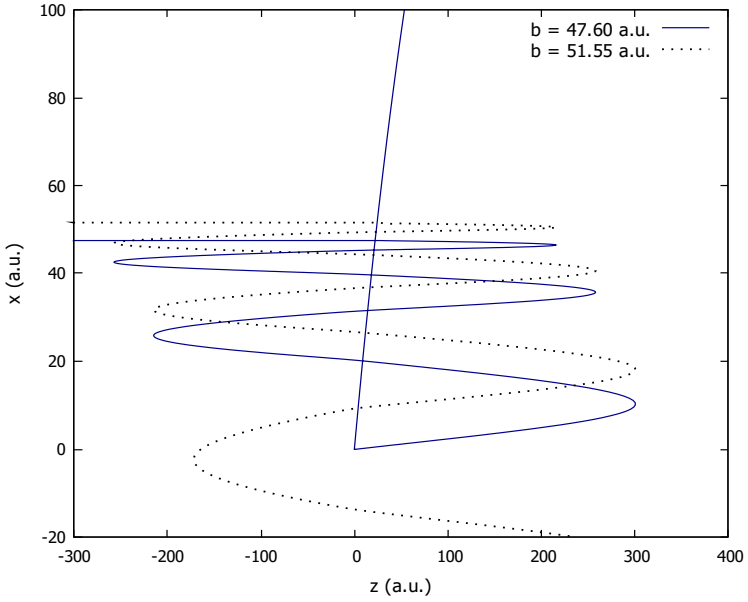

FIG. 5: Electron trajectories for two impact parameters, $b = 47.60$ (solid curve) and 51.55 a.u. (dotted curve).

first corresponds to a large probability $P = 0.14 \times 10^{-4}$ a.u. and the second to a small probability $P = 0.42 \times 10^{-8}$ a.u. Both trajectories undergo Coulomb focusing. However, whereas the first trajectory approaches very close to the Coulomb center (minimum distance

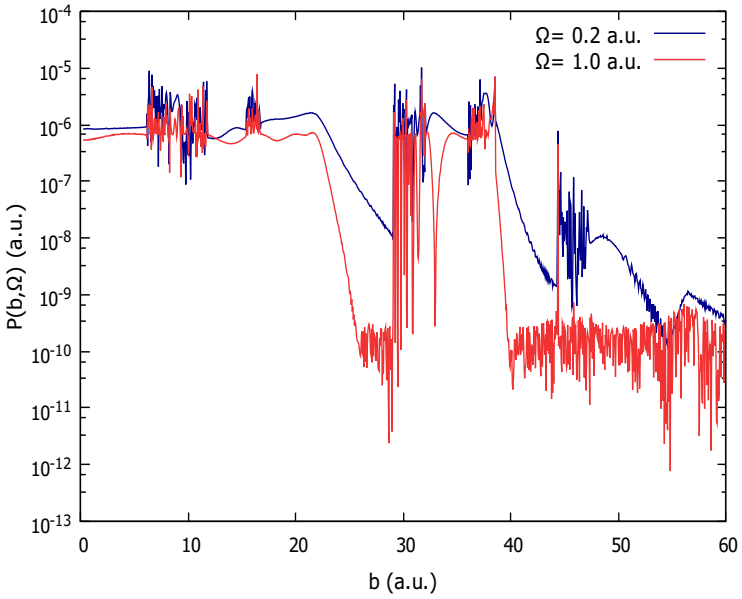

FIG. 6: $P(b,\Omega)$ as a function of the impact parameter b for the case, $Z = 1$, $v = 0.1$ a.u. $F_0 = 0.05338$ a.u. ($I = 100$ TW/cm^2), $\omega = 0.1$ a.u., and $\Omega = 0.2$ a.u. (upper curve) and 1.0 a.u. (lower curve)

0.0164 a.u.), the second trajectory misses the center (the closest approach is 9.24 a.u.) and does not exhibit a large acceleration, therefore contributing very little to the radiation. Therefore the spikes in P as a function of b correspond to the hard-collision trajectories. Apparently the hard-collision events depend randomly on the impact parameter b and lead to the fractal structure.

However, two certain features can be noticed. First, in intermediate range of impact parameters the spikes exhibit a quasiperiodic structure. Second, due to the initial nonzero velocity in the z direction, trajectories drift in this direction leading to the disappearance of spikes and the effective cut-off in b. For the given choice of the parameters this occurs at about 140 a.u.

To give a rough analytical estimate for the cut-off in b, consider the drift of the electron in the direction perpendicular to the electric field with the starting position $x = b$, $z = 0$. Neglecting z as compared to x during the drift, we obtain for the drift velocity v_x

$$v_x = \left[2Z\left(\frac{1}{x} - \frac{1}{b}\right)\right]^{1/2}.$$

Integrating the equation

$$\frac{dx}{dt} = v_x(x)$$

we obtain the expression for the time during which the electron reaches the Coulomb center

$$t = \pi \left(\frac{b^3}{8Z}\right)^{1/2}$$

During this time the center of the trajectory in the z direction covers the distance

$$z_0 = v_0 t = \pi v_0 \left(\frac{b^3}{8Z}\right)^{1/2}.$$

In order to obtain a hard collision, this distance should be smaller than the oscillating amplitude in the z direction F_0/ω^2. As a result, we obtain for the impact parameter cut-off

$$b < (8Z)^{1/3} \left(\frac{F_0}{\pi v_0 \omega^2}\right)^{2/3}.$$

This estimate works well when the quivering amplitude is large compared to the impact parameter. For example in case $F_0 = 0.05338$, $\omega = 0.0147$, $b < 170$ a.u. which agrees very well with data presented in Fig. 3.

According to this estimate, with the growth of ω the cut-off impact parameter should decrease as $\omega^{-4/3}$. In Fig. 6 we show $P(b)$ for $\omega = 0.1$ a.u. ($\lambda = 456$ nm), $\Omega = 0.2$ and 1.0 a.u. The reduction of the impact parameter cut-off value is qualitatively confirmed by the figure, although it is not as drastic as predicted by the $\omega^{-4/3}$ dependence. Since the quivering length in this case is 5.34 a.u., the above estimate is not working as well. Another apparent features in this case are that the spike structure is not as regular, and in the range of impact parameters where P is substantial, it is larger than in the case $\omega = 0.0147$. Another interesting feature is that the fractal structure of $P(b)$ dependence extends well beyond the quivering length l. Apparently the fractal structure in the present problem is a more general feature than suggested in [27].

To investigate the role of the constant phase shift φ_0, consider the z-component of the electron velocity in the absence of the Coulomb interaction

$$v_z = v_0 - \frac{F_0}{\omega}\sin\varphi_0 + \frac{F_0}{\omega}\sin(\omega t + \varphi_0).$$

To obtain Coulomb focusing, we need a relatively small averaged velocity

$$\bar{v}_z = v_0 - \frac{F_0}{\omega}\sin\varphi_0$$

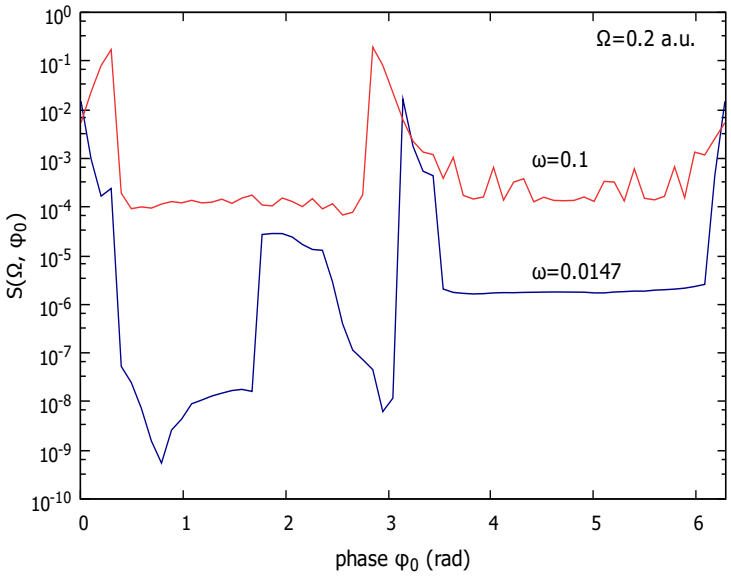

FIG. 7: Total bremsstrahlung cross section per unit frequency, Eq. (4), for $F_0 = 0.0538$, $\Omega = 0.2$ a.u. as a function of phase φ_0 for two values of the laser frequency.

For the case of field parameters $F_0 = 0.05338$, $\omega = 0.0147$ presented in Fig. 3, this occurs in two narrow ranges of φ_0 close to 0 and π. For all other phases the electron simply does not get close to the Coulomb center, and the radiation is weak. This is demonstrated in Fig. 7 for two values of laser frequencies corresponding to $v_0\omega/F_0 = 0.0275$ and 0.1873 a.u. This figure also demonstrates the chaotic structure in the dependence of P on the other initial parameter, φ_0.

We conclude that the average over φ_0 strongly reduces the cross section for larger value of the quiver velocity $F_0/\omega = 3.63$ a.u., but not as strongly for a smaller $F_0/\omega = 0.534$ a.u. In Fig. 8 we compare the bremsstrahlung cross section for $\varphi_0 = 0$ with the averaged cross section for the first case. Although the averaging decreases the result by an order of magnitude, the bremsstrahlung process is still much more efficient than in the $F_0 = 0$ case. To show this, we have calculated the field-free bremsstrahlung cross section for electron velocity 3.56 a.u. (kinetic energy 6.35 a.u.), the same as chosen for plotting field-free $P(b, \Omega)$ in Fig. 3. The figure shows that the field-free cross section is about two orders of magnitude lower than the averaged cross section for the laser-assisted process.

To expand the Coulomb focusing to a larger range of φ_0, the quiver velocity should be made comparable to v_0. This can be achieved by reducing F_0 or increasing frequency. To

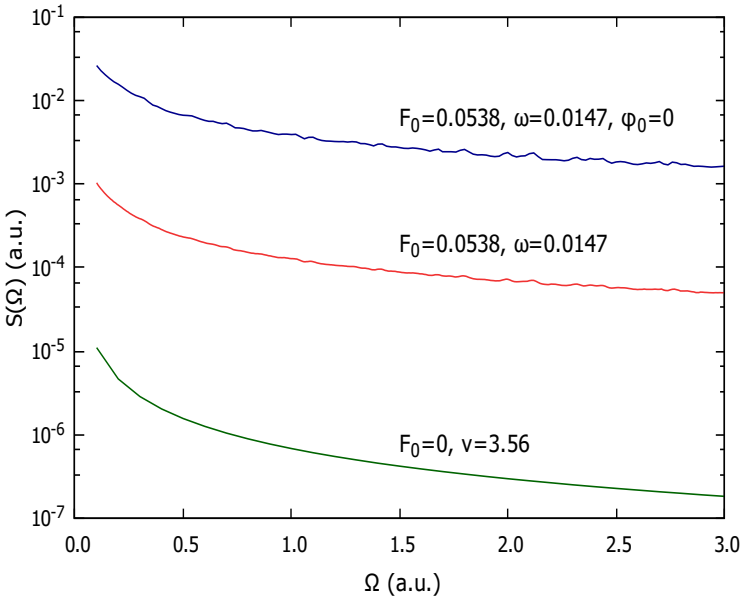

FIG. 8: Total bremsstrahlung cross section per unit frequency, Eq. (4), for $\varphi_0 = 0$ and averaged over φ_0. The field-free cross section is given for velocity $v_0 = 3.56$ a.u.

demonstrate this, we choose $\omega = 0.05696$ ($\lambda = 800$ nm) and $F_0 = 0.0056$ a.u. ($I = 1.1$ TW/cm^2). For these field parameters, however, the ponderomotive energy is small, $E_p = 2.4 \times 10^{-3}$ a.u., therefore, with the initial electron velocity $v_0 = 0.1$ a.u., only infrared photons (with the wavelength about 5 μm or longer) will be emitted. Instead of the high-order harmonic generation, we obtain frequencies that are lower than those we are starting with. To increase the frequency range, we need to increase the initial velocity to a few a.u., but then the laser-assisted bremsstrahlung would become indistinguishable from the field-free bremsstrahlung. Nevertheless, we will investigate the case of low v_0 and low Ω since it is closely connected to the interesting problem of chaos in ionization of Rydberg atoms by microwave and far infrared radiations.

With these field parameters, in a certain range of impact parameters within the chaotic regime, we found unstable trajectories which become trapped by the Coulomb field. To demonstrate this, in Fig. 9 we present the electron distance from the Coulomb center as a function of time for several impact parameters.

As follows from this figure, the capture event randomly depends on b and can occur for small b, as well as for large b. Trajectories for these two cases are shown in Fig. 10. Similar pictures were obtained by Wiesenfeld [28]. For the bremsstrahlung problem, the important

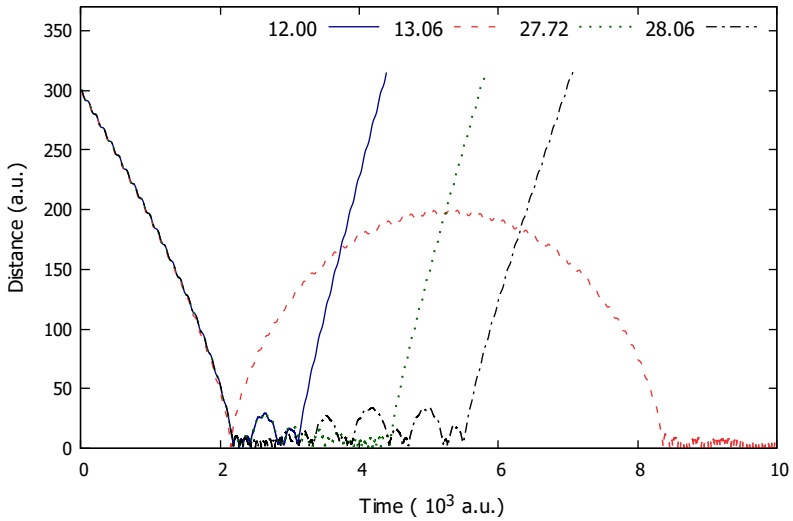

FIG. 9: Electron distance from the Coulomb center as a function of time for several impact parameters, $\omega = 0.05696$, $F_0 = 0.0056$ a.u., $\varphi_0 = 0$.

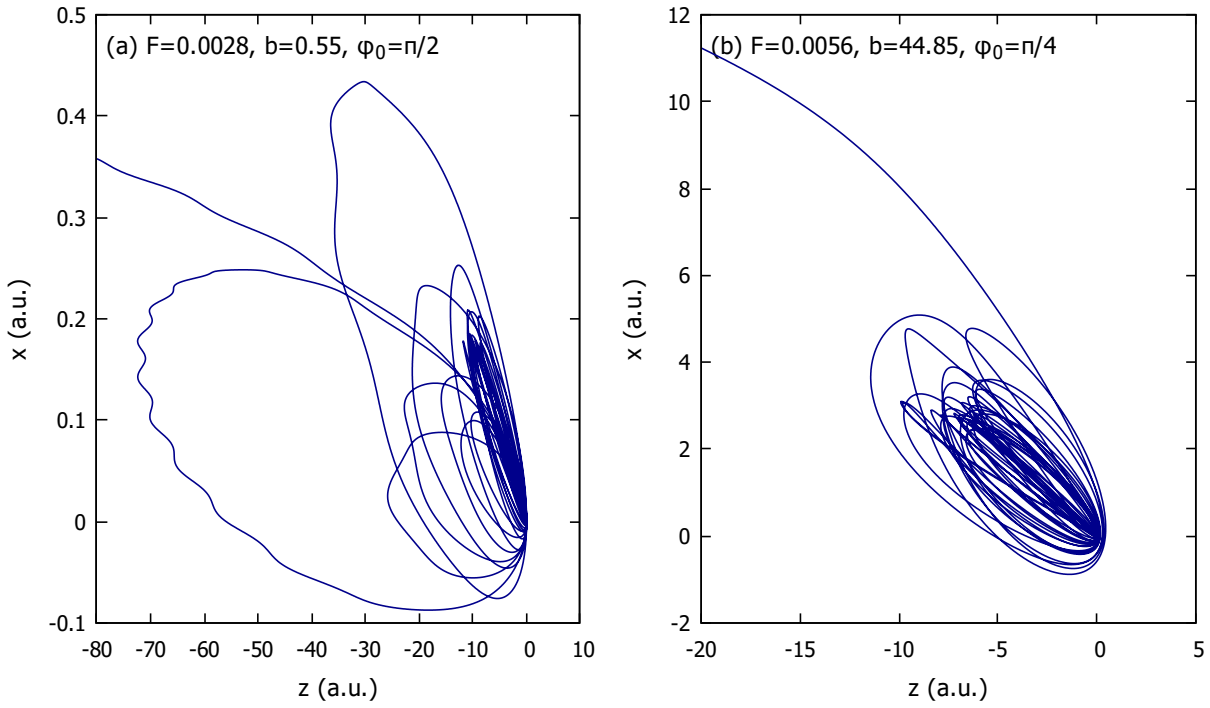

FIG. 10: Electron trajectory for; (a) $\omega = 0.05696$, $F = 0.0028$, $b = 0.55$, $\varphi_0 = \pi/2.$, (b) $\omega = 0.05696$, $F_0 = 0.0056$, $b = 44.85$, $\varphi_0 = \pi/4$.

quantity is the closest approach where the most radiation occurs. To demonstrate the relevant fractal structure, we plot in Fig. 11 the distance as a function of time in the vicinity of $b = 27.75$ a.u. with the successive enlargement of the b scale.

The fractal structure of the radiation probability as a function of b leads to computational difficulties in calculation of the total bremsstrahlung cross section. Another difficulty is of the physical origin. Some of the orbits within the chaotic region remain trapped for a long time, sometimes probably forever corresponding to the invariant tori found by Leopold and Percival [29] (trajectories of class C1) in the classical ionization problem. In the classical treatment, the electron in trapped orbits will radiate an infinite energy, even if the electron energy loss due to radiation is incorporated in the equations of motion, and the cross section will become infinite. It is apparent that the classical treatment fails at this point, and quantum effects should be incorporated. Fortunately, however, for a typical calculation covering an extended range of impact parameters b there are very few trajectories which are trapped "forever", and they can be simply neglected in calculation of the radiation cross section. The error due to this omission is substantially smaller than the error caused by the fractal structure of the dependencies of P on b and φ_0. In Fig. 12 we present the dependence of the radiation cross section on φ_0. The result of averaging over φ_0 depends on the increment $\Delta\varphi_0$ used for representing dependence $S(\varphi_0)$. In Table I we present the result of the average using the trapezoidal rule with various $\Delta\varphi_0$. This comparison allows us to claim that the uncertainty in S due to the chaotic behavior of trajectories is about 0.4%

Finally, in Fig. 13 we present the bremsstrahlung cross section for $\varphi_0 = 0$ and the cross section averaged over φ_0. A substantial enhancement of radiation as compared to the $F_0 = 0$ case is observed. This case contrasts with the large quivering length case presented in Fig. 8 where the averaging over φ_0 substantially cancels the enhancement effect due to the Coulomb focusing.

V. LIMITATION OF THE MODEL AND QUANTUM EFFECTS

There are two important features which are not observed in the present calculations, both related to the resonance effects. The first type of the resonance occurs when the frequency of the emitted radiation Ω is equal to or close to $s\omega$ where s is a positive integer. The

TABLE I: Dependence of the averaged cross section on the increment $\Delta\varphi_0$

$\Delta\varphi_0$	$\omega = 0.002$	$\omega = 0.01$
$\pi/16$	0.3476	0.1783
$\pi/32$	0.3499	0.1784
$\pi/64$	0.3498	0.1780

other type of resonance is related to a temporary capture of the electron by the ion with the following ionization. In fact the second type includes the first type as well since the number of absorbed photons before the capture k is related to the energy of the bound state ϵ and the frequency of the emitted radiation as [16]

$$\Omega = E_0 - \epsilon + k\omega.$$

The total number of absorbed photons is $k+m$ where m is the number of absorbed photons after the capture.

Both effects were described in the past by quantum-mechanical methods [7–9, 12, 16]. Description of the first effect does not seem to be possible by the pure classical theory since the dependence $\mathbf{r}(t)$ does not contain higher harmonics with frequencies $s\omega$. Quantal description which takes into account electron-laser interaction in higher orders is essential in this case. It is interesting, however, that the stimulated bremsstrahlung which is the emission of s photons of frequency ω can be described semiclassically [42] by treating electron motion classically but the electromagnetic field quantum-mechanically. This suggests that the classical-trajectory approach used in the present paper can be modified to treat resonances of the first type. Resonances of the second type can be obtained in the classical ionization problem [43, 44] when the process starts with the stationary orbit. In the scattering problem the temporary capture does occur in classical theory. However, the motion in quasistable orbits occurs usually for a few impact parameters, therefore the sharp enhancements observed in $P(b,\Omega)$ do not show up in the $S(\Omega)$ dependence. Nevertheless it is useful to discuss classical-quantum-mechanical correspondence for the resonant scattering.

The quantum-mechanical description of the resonant scattering [16] in the case of Coulomb potential is particularly challenging because of the large number of Rydberg states. It was assumed [16] that the capture occurs only in the ground state of the hydrogen atom

because the field-free radiative recombination cross section is higher for this state. However, the presence of the ac field may radically change this situation. In fact the classical quasistable quasiperiodic orbits in which capture occurs, according to the correspondence principle, represent a superposition of these Rydberg states. The problem with the classical treatment is that it might result in an infinite radiation in this case, if the orbit is not ionized classically. There are two quantum effects responsible for the finite radiation probability. One is the stimulated and spontaneous emission leading to electron transition to a lower quantum state, typically to the atomic ground state. The other is the multiphoton or tunneling ionization resulting in electron escape from the orbit. Our simulations have shown that typically electron is captured either into a high-lying orbit which ionizes quickly classically (trajectory of class C3 according to Leopold and Percival [29]), or in a lower orbit with the energy roughly corresponding to that of the $n = 2$ or $n = 3$ states. The latter, as a rule, is an invariant torus, and often never ionizes within the classical mechanics domain [29]. Its decay should be described quantum-mechanically. The lifetime of the corresponding $n = 2$ quantum state with respect to the spontaneous emission to the ground state (6.6×10^7 a.u.) is too long compared to our typical time scale, and the stimulated emission can be neglected in nonresonant case, that is if $s\omega$, $s = 1, 2, ...$ is not close to the transition frequency, 0.375 a.u. Therefore the major contribution to the decay of the intermediate state is due to the multiphoton or tunneling ionization. Our typical field parameters correspond to the multiphoton regime (large Keldysh parameter), and the ionization rate can be estimated by the semiclassical perturbation theory [45], since our intensity is relatively small. At $I = 1.1$ TW/cm^2, $\lambda = 800$ nm ionization of the $n = 2$ manifold is dominated by the three-photon absorption with the rate 0.6×10^{-4} a.u. Although the corresponding lifetime is compatible with our time scale, the problem remains with quasistable trajectories for which the electron passes the nucleus many times during the time interval of 10^4 a.u. In the classical theory the radiation probability is strongly increased due to these passages whereas the quantum state corresponding to the quasistable orbit does not radiate at all (or radiates on a much longer time scale due to the spontaneous emission). Fortunately, as was discussed above, for each particular value of the initial phase φ_0 there are very few impact parameters leading to quasistable trajectories. Therefore these cases are simply ignored when we integrate over the impact parameter to obtain the cross section. The chaotic behavior of the trajectories, discussed above, in large extent smears out the uncertainty created by this approach.

One more deficiency of the classical approach is that it does not provide the high-frequency cut-off, the cross section is simply monotonically decreasing with Ω. However, from the discussion above, it can be estimated as $v_0^2/2+2E_p$ since this is the maximum kinetic energy of the electron at the distance of a few Bohr from the Coulomb center. More accurate quantum-mechanical treatment [16] suggests that the cut-off frequency is greater than the above estimate by $\mathbf{F}\cdot\mathbf{v}_0/\omega$, or Fv_0/ω in case of initial velocity parallel to the ac field. However, for the cases discussed in the present paper this is an insignificant extension. For example, if $I = 100$ TW/cm^2, $\omega = 0.0147$ a.u. this estimate extends the cut-off frequency from 6.6 to 6.96 a.u.

VI. CONCLUSION

We conclude that the Coulomb focusing, leading to a substantial extension of the impact parameters contributing to the bremsstrahlung cross section, results in a substantial increase (by one to two orders of magnitude) of the cross section as compared to the pure Coulomb case. Due to chaotic scattering in the combined Coulomb and ac fields, the emission probability $P(b,\Omega,\varphi_0)$ as a function of b and the constant phase of the laser field φ_0 exhibits fractal structures. However, these structures are smeared out when the cross section is integrated over b and averaged over φ_0. The average over φ_0 is completely equivalent to the average over the starting point of trajectory [7]. Although the accuracy of the classical calculations is good, they do not include the resonance regime studied quantum-mechanically in [7–9, 16]. These studies were concentrating on the regime whereby the initial electron kinetic energy is high compared to the ponderomotive energy E_p. In contrast, the present paper is focused on the case of small initial kinetic energy but relatively high E_p when the Coulomb focusing effects become important.

To address the question about the connection with previous quantum-mechanical calculations, we note that nonperturbative quantal treatments were applied so far only to short-range potentials. Therefore previous quantal calculations and the present one complement each other rather than present two approaches to the same problem. Refs. [16,17], for example, concentrate on the short-range case when quantum-mechanical effects are important. Although those calculations include some effects of the Coulomb potential, they are mostly pertinent to quantities responsible for the resonant capture, for example, radiative

recombination cross section. In contrast, we are mostly concerned with the effect of the Coulomb interaction in the continuum, particularly the Coulomb focusing effect, which can be described classically, as follows, for example, from Refs. [18-25]. It would be unphysical to apply our approach to a short-range potential, since quantum effects play a crucial role in scattering of low-energy electrons by a short-range potential.

As has been demonstrated, agreement between classical and quantum approach to the bremsstrahlung in the Coulomb field is good for electron velocities considered in the present paper. Relativistic effects and interference of classical trajectories might be nonnegligible, but we believe that we have demonstrated that the nonrelativistic classical approach captures the major features of the problem.

The bremsstrahlung process discussed in the present paper can be of interest for the purpose of generation of UV photons. Whereas the standard HHG process, starting from the bound state, has an advantage of a more focused electron current, the continuum-continuum transition might be efficient due to a broad range of impact parameters contributing to the radiation. The efficiency can be increased further by increasing the ion charge Z. Another possibility is changing the geometry by choosing a nonzero angle between the direction of the incident beam and the laser polarization. Changing the polarization from linear to circular and elliptical can be also explored.

Acknowledgments

The authors are grateful to Misha Frolov for stimulating discussions. This work was supported by the US National Science Foundation under Grant No. PHY-1803744.

APPENDIX A: MODIFIED BESSEL FUNCTION OF THE THIRD KIND

Consider the function $K_{i\mu}(x)$ where μ and x are real. It satisfies the equation

$$x^2 y'' + xy' - (x^2 - \mu^2)y = 0$$

By substitution

$$y = x^{-1/2} f(x)$$

we obtain

$$f'' + \left(-1 + \frac{\mu^2 + 1/4}{x^2}\right) f = 0.$$

We treat this equation in the spirit of the quasiclassical approximation. Since the x interval is between 0 and ∞, we introduce the Langer correction. Then, what can be called the square of the momentum, is

$$k^2(x) = -1 + \frac{\mu^2}{x^2}.$$

For $x > \mu$ (classically forbidden region) the action, or the phase integral, is

$$S(x) = \int_\mu^x \left(1 - \frac{\mu^2}{(x')^2}\right)^{1/2} dx' = (x^2 - \mu^2)^{1/2} - \mu \arccos\frac{\mu}{x}.$$

Using the uniform Airy function approximation [46], we obtain

$$K_{i\mu}(x) = \frac{c}{(x^2 - \mu^2)^{1/4}} \left(\frac{3}{2}S\right)^{1/6} \mathrm{Ai}\left[\left(\frac{3}{2}S\right)^{2/3}\right]. \tag{A1}$$

The constant can be determined from the asymptotic expression for $K_{i\mu}(x)$

$$K_{i\mu}(x) \sim \left(\frac{\pi}{2x}\right)^{1/2} e^{-x}.$$

Using now the asymptotic of the Airy function for $x \gg \mu$,

$$S(x) \sim x - \mu\pi/2, \qquad \left(\frac{3}{2}S\right)^{1/6} \mathrm{Ai}\left[\left(\frac{3}{2}S\right)^{2/3}\right] \sim \frac{1}{2\pi^{1/2}} e^{-S}$$

we obtain

$$c = 2^{1/2}\pi e^{-\pi\mu/2}.$$

For $x < \mu$ (classically allowed region) we obtain the same expression (A1) except that now

$$S(x) = \int_x^\mu \left(-1 + \frac{\mu^2}{(x')^2}\right)^{1/2} dx' = -(\mu^2 - x^2)^{1/2} + \mu \ln\frac{\mu + (\mu^2 - x^2)^{1/2}}{x}$$

and the argument of the Airy function is negative.

In summary

$$K_{i\mu}(x) = \frac{\pi 2^{1/2}}{|\mu^2 - x^2|^{1/4}} e^{-\pi\mu/2} \left(\frac{3}{2}S\right)^{1/6} \mathrm{Ai}\left[\pm\left(\frac{3}{2}S\right)^{2/3}\right]$$

where the sign of the argument of Airy function is + for $x > \mu$ and − for $x < \mu$.

This expression works even at the turning point, when $x = \mu$. Suppose, for example, that x approaches μ from below so that $\mu - x$ is a small number. Then

$$S(x) = \int_x^\mu \frac{(\mu^2 - y^2)^{1/2}}{y} dy = \int_0^{\mu - x} \frac{[\mu^2 - (\mu - \eta)^2]^{1/2}}{\mu - \eta} d\eta.$$

In the limit $x \to \mu$ we obtain

$$S(x) \approx \frac{(2\mu)^{1/2}}{\mu} \int_0^{\mu-x} \eta^{1/2} d\eta = \frac{2}{3} \left(\frac{2}{\mu}\right)^{1/2} (\mu - x)^{3/2}$$

and

$$\frac{\left(\frac{3}{2}S\right)^{1/6}}{(\mu^2 - x^2)^{1/4}} = 2^{-1/6} \mu^{-1/3}.$$

Finally

$$K_{i\mu}(\mu) = \pi \left(\frac{2}{\mu}\right)^{1/3} e^{-\pi\mu/2} \mathrm{Ai}(0) \tag{A2}$$

where $\mathrm{Ai}(0) = 0.35502805$

As an example, consider the cross section $S(\Omega)$ in the case of large frequency Ω when $\mu \gg 1$. Using Eq. (A2)

$$e^{\pi\mu/2} K_{i\mu}(\mu) = \pi \left(\frac{2}{\mu}\right)^{1/3} \mathrm{Ai}(0)$$

and a similar equation for the derivative

$$e^{\pi\mu/2} K'_{i\mu}(x) = \frac{\pi 2^{1/2} |\mu^2 - x^2|^{1/4}}{x} \left(\frac{3}{2}S\right)^{-1/6} \mathrm{Ai}' \left[\pm \left(\frac{3}{2}S\right)^{2/3}\right]$$

$$e^{\pi\mu/2} K'_{i\mu}(\mu) = \pi \left(\frac{2}{\mu}\right)^{2/3} \mathrm{Ai}'(0),$$

we obtain

$$e^{\pi\mu} K_{i\mu}(\nu) K'_{i\mu}(\mu) = \frac{2\pi^2}{\mu} \mathrm{Ai}(0)\mathrm{Ai}'(0) = -\frac{\pi}{3^{1/2}\mu}$$

where we have used

$$\mathrm{Ai}(0)\mathrm{Ai}'(0) = -\frac{1}{2\pi\sqrt{3}}.$$

Finally

$$S(\Omega) = \frac{16\pi Z^2}{3^{3/2}(mv_0)^2 c^3 \Omega}$$

meaning that the effective radiation $\Omega S(\Omega)$ is independent of Ω at high Ω. This equation is the same as in [32], Eq. (70.22) which was obtained there by other methods.

APPENDIX B: REGULARIZED COULOMB TRAJECTORIES

In cylindrical coordinates, consider the following Hamiltonian for the motion of the electron in Coulomb plus external electric field,

$$H(\rho, z, p_\rho, p_z, t) = \frac{1}{2}[p_\rho^2 + p_z^2] + \frac{L_z^2}{2\rho^2} - \frac{Ze^2}{\sqrt{\rho^2 + z^2}} - F_0 z \cos(\omega t + \varphi_0), \tag{B1}$$

where L_z is the $z-$component of the electron's angular momentum and Z is the charge of the Coulomb center. The numerical solutions for the equations of motion near the Coulomb center become highly unstable due to the singularity in the potential. In this appendix, we will show how to remove this singularity from the Hamiltonian and obtain *regularized* Coulomb trajectories based on the formalism of extended Hamiltonian.

1. Extended Hamiltonian

The ordinary Hamiltonian H can be extended to a new Hamiltonian Γ by introducing time as a new mechanical variable [47]. The extended Hamiltonian Γ can be written as

$$\Gamma = H + p_t, \tag{B2}$$

where p_t is the canonical momentum for time t. In the extended phase space, two additional Hamilton's equations are defined according to

$$\frac{dt}{d\tau} = \frac{\partial \Gamma}{\partial p_t} = 1, \tag{B3}$$

$$\frac{dp_t}{d\tau} = -\frac{\partial \Gamma}{\partial t} = -\frac{\partial H}{\partial t}, \tag{B4}$$

where τ now works as the independent variable. It can be readily shown that $p_t(t) = -H(t)$ and for a time independent Hamiltonian, $p_t(t) = -E_0$, with E_0 being the initial energy of the system. Thus, $\Gamma(\tau = t) = 0$.

2. Regularization of the extended Hamiltonian

For the purpose of regularization, we will introduce the semi-parabolic coordinates into the extended Hamiltonian, according to [28]

$$\chi = \sqrt{\sqrt{\rho^2 + z^2} + z}, \quad \eta = \sqrt{\sqrt{\rho^2 + z^2} - z}, \quad \chi, \eta \geq 0. \tag{B5}$$

Now the extended Hamiltonian in semi-parabolic coordinates will read,

$$\Gamma(\chi, \eta, t, p_\chi, p_\eta, p_t) = \frac{1}{2}(\chi^2 + \eta^2)(p_\chi^2 + p_\eta^2) + \frac{L_z^2}{2\chi^2\eta^2} - \frac{2Ze^2}{\chi^2 + \eta^2} - \frac{1}{2}(\chi^2 - \eta^2)F_0 \cos(\omega t + \varphi_0) + p_t$$

As the next step towards the regularization, the old extended Hamiltonian is transformed to a new Hamiltonian K together with a time transformation. This is achieved via the

following rule

$$K = g(\chi,\eta)\Gamma, \quad dt = g(\chi,\eta)dT. \tag{B6}$$

It can be shown that the canonical nature of the equations of motion is preserved in the new Hamiltonian K [48]. For the Coulomb problem in semi-parabolic coordinates, the choice of $g(\chi,\eta) = \chi^2+\eta^2$ will eliminate the singularity at $(\rho = 0, z = 0)$ from the Coulomb potential. The transformed Hamiltonian $K(\chi,\eta,t,p_\chi,p_\eta,p_t)$ for the extended Hamiltonian Γ is given by

$$K = \frac{1}{2}(p_\chi^2+p_\eta^2) + \frac{L_z^2}{2\chi^2} + \frac{L_z^2}{2\eta^2} + (\chi^2+\eta^2)p_t - 2Ze^2 - \frac{1}{2}(\chi^4-\eta^4)F_0\cos(\omega t+\varphi_0). \tag{B7}$$

Now, the Hamilton's equations of motion for K are as follows (here we have assumed for simplicity $L_z = 0$):

$$\frac{dt}{dT} = \chi^2+\eta^2 \tag{B8}$$

$$\frac{dp_t}{dT} = -\frac{1}{2}[\chi^4-\eta^4]F_0\omega\sin(\omega t+\varphi_0) \tag{B9}$$

$$\frac{d^2\chi}{dT^2} = 2\chi^3F_0\cos(\omega t+\varphi_0) - 2\chi p_t \tag{B10}$$

$$\frac{d^2\eta}{dT^2} = -2\eta^3F_0\cos(\omega t+\varphi_0) - 2\eta p_t \tag{B11}$$

And the initial conditions at $T = 0$ are

$$t = t_0,\ p_t = -H(t_0),\ \frac{d\chi_0}{dT} = \eta_0\dot\rho_0 + \chi_0\dot z_0,\ \frac{d\eta_0}{dT} = \chi_0\dot\rho_0 - \eta_0\dot z_0,$$

where (ρ_0, z_0, t_0) and $(\dot\rho_0, \dot z_0)$ are initial configuration and velocities in the (ρ, z, t) coordinates. The numerical solutions of Eqs. (B8)-(B11) behave well near the Coulomb center. By tabulating the solutions $\chi(T), \eta(T)$ and $t(T)$, the trajectory in (ρ, z, t) coordinates can be numerically obtained.

APPENDIX C: CALCULATION OF FOURIER INTEGRALS

For calculation of Fourier transform of Cartesian components of acceleration, Eq. (1), we use the grid points obtained from the regularized Coulomb trajectories method, Appendix

B. Assuming that the values of a function $f(t)$ is varying slowly between two successive grid points t_1, t_2, we can approximate it by a linear function

$$f(t) = f_0 + \beta t$$

where

$$\beta = \frac{f_2 - f_1}{t_2 - t_1}, \qquad f_0 = f_1 - \beta t_1.$$

then

$$\int_{t_1}^{t_2} f(t) e^{i\Omega t} dt = \left(\frac{f_0}{i\Omega} + \frac{\beta}{\Omega^2} \right) (e^{i\Omega t_2} - e^{i\Omega t_1}) + \frac{\beta}{i\Omega} (t_2 e^{i\Omega t_2} - t_1 e^{i\Omega t_1}).$$

However, close to the nucleus the acceleration varies very rapidly and the linear approximation is insufficient. In this case the integration of acceleration can be reduced to the integration of velocity. Consider the time interval between t_1 and t_2 where acceleration cannot be approximated by a linear function. Then

$$\int_{t_1}^{t_2} \frac{dv}{dt} e^{i\Omega t} dt = v(t_2) e^{i\Omega t_2} - v(t_1) e^{i\Omega t_1} - i\Omega \int_{t_1}^{t_2} v(t) e^{i\Omega t} dt. \tag{C1}$$

If necessary, this can be reduced further to integration of the coordinate

$$\int_{t_1}^{t_2} \frac{dv}{dt} e^{i\Omega t} dt = [v(t_2) - i\Omega x(t_2)] e^{i\Omega t_2} - [v(t_1) - i\Omega x(t_1)] e^{i\Omega t_1} - \Omega^2 \int_{t_1}^{t_2} x(t) e^{i\Omega t} dt. \tag{C2}$$

Note, however, that for numerical calculations it is not convenient to reduce the whole integration to the integral of velocity or coordinate (as is done in the analytically-solvable Coulomb case [32]) because these quantities do not disappear at $t \to \pm\infty$. Generally even acceleration does not disappear in this limit because of the ac field. However, since

$$\int_{-\infty}^{\infty} e^{i\Omega t} F_0 \cos(\omega t + \varphi_0) dt = \pi F_0 e^{-i\varphi_0} \delta(\Omega - \omega)$$

this contribution can be dropped unless $\omega = \Omega$. In numerical calculations the contribution of the ac field term should be included because it influences the integrals in Eqs. (C1) and (C2). Therefore we subtract the following expression from the numerical result

$$\int_0^{t_f} e^{i\Omega t} F_0 \cos(\omega t + \varphi_0) dt = \frac{F_0}{2} \left[e^{i\varphi_0} \frac{e^{i(\Omega+\omega)t_f} - 1}{i(\Omega + \omega)} + e^{-i\varphi_0} \frac{e^{i(\Omega-\omega)t_f} - 1}{i(\Omega - \omega)} \right]$$

where we have assumed that the initial integration time is 0 and the final integration time is t_f.

Fig. 14 demonstrates the importance of the above correction, Eq. (C1). We present here the probability per unit frequency $P(b, \Omega)$, Eq. (3), as a function of the impact parameter

b for a pure Coulomb field. When we employ Eq. (C1) at the distance of 20 integration points from the closest approach, we obtain perfect agreement with the exact result, Eq. (6). Otherwise we observe a divergence at low impact parameters.

---

[1] M. V. Fedorov and R. V. Karapetyan, J. Phys. A **9**, L103 (1976).

[2] A. V. Borisov and V. Ch. Zhukovskii, Zh. Eksp. Teor. Fiz. **70**, 477 (1976) [Sov. Phys. JETP **43**, 247 (1976)].

[3] R. V. Karapetyan and M. V. Fedorov, Kvant. Electron. **4**, 2203 (1977) [Sov. J. Quantum Electron. **7**, 1260 (1977)].

[4] R. V. Karapetyan and M. V. Fedorov, Zh. Eksp. Teor. Fiz. **75**, 816 (1978) [Sov. Phys. JETP **48**, 412 (1978)].

[5] A. V. Borisov, V. Ch. Zhukovskii, and P. A. Eminov, Zh. Eksp. Teor. Fiz. 78, 530 (1980) [Sov. Phys. JETP **51**, 267 (1980)].

[6] V. P. Krainov and S. P. Roshchupkin, Zh. Eksp. Teor. Fiz. **84**, 1302 (1983) [Sov. Phys. JETP **57**, 754 (1983)].

[7] M. V. Fedorov and M. Yu. Ivanov, Laser Physics **3**, 365 (1993).

[8] F. Zhou and L. Rosenberg, Phys. Rev. A **48**, 505 (1993).

[9] R. Daniele and E. Fiordilino, Il Nuovo Cimento D **18**, 547 (1996).

[10] M. V. Fedorov *Atomic and Free Electrons in a Strong Laser Field*, World Scientific, Sngapore, 1997.

[11] F. Ehlotzky, A. Jaron, and J. Z. Kaminski, Phys. Rep. **297**, 63 (1998).

[12] A. Florescu and V. Florescu, Phys. Rev. A **61**, 033406 (2000).

[13] E. Lötstedt, U. D. Jentschura, and C. H. Keitel, Phys. Rev. Lett. **98**, 043002 (2007).

[14] S. Schnez, E. Lötstedt, U. D. Jentschura, and C. H. Keitel, Phys. Rev. A **75**, 053412 (2007).

[15] A. A. Lebed' and S. P. Roshchupkin, Phys. Rev. A **81**, 033413 (2010).

[16] A. N. Zheltukhin, A. V. Flegel, M. V. Frolov, N. L. Manakov, and A. F. Starace, Phys. Rev. A **89**, 023407 (2014).

[17] A. N. Zheltukhin, A. V. Flegel, M. V. Frolov, N. L. Manakov, and A. F. Starace, J. Phys. B **48** 075202 (2015).

[18] Th. Brabec, M. Yu. Ivanov, and P. B. Corkum, Phys. Rev. A **54** R2551 (1996).

[19] G. L. Yudin and M. Y. Ivanov, Phys. Rev. A **63**, 033404 (2001).

[20] D. Comtois, D. Zeidler, H. Pépin, J. C. Kieffer, D. M.Villeneuve, and P. B. Corkum, J. Phys. B **38**, 1923 (2005).

[21] D. Shafir, H. Soifer, C. Vozzi, A. S. Johnson, A. Hartung, Z. Dube, D. M. Villeneuve, P. B. Corkum, N. Dudovich, and A. Staudte, Phys. Rev. Lett. **111**, 023005 (2013).

[22] S. A. Berman, C. Chandre, and T. Uzer, Phys. Rev. A **92**, 023422 (2015).

[23] C. Huang, Q. Liao, Y. Zhou, and P. Lu, Optics Express **18**, 14293 (2010).

[24] J. Daněk, K. Z. Hatsagortsyan, and Ch. H. Keitel, Phys. Rev. A **97**, 063410 (2018).

[25] J. Lu, Q. Li, L. He, and H. Qiao, J. Phys. B **52**, 035401 (2019).

[26] L. D. Landau and E. M. Lifshitz, *Quantum Mechanics (Nonrelativistic Theory)* (Pergamon, Oxford, 1977).

[27] L. Wiesenfeld, Phys. Lett. A **144**, 467 (1990).

[28] L. Wiesenfeld, Acta Phys. Polonica B **23**, 271 (1992)

[29] J. G. Leopold and I. C. Percival, J. Phys. B: At. Mol. Phys. **12**, 709 (1979).

[30] U. Smilansky, The classical and quantum theory of chaotic scattering, in: *Chaos and Quantum Physics*, eds. M. J. Gianonni, A. Voros and J. Zinn-Justin, p. 371. (Elsevier, Amsterdam, 1991).

[31] E. J. Heller, Wavepacket dynamics and quantum chaology, *ibid.*, p. 547.

[32] L. D. Landau and E. M. Lifshitz, *The Classical Theory of Fields: Course of Theoretical Physics, Volume 2*, 3rd ed. (Pergamon, Oxford, 1971).

[33] V. B. Berestetskii, L. P. Pitaevskii, E. M. Lifshitz, *Quantum Electrodynamics: Volume 4 (Course of Theoretical Physics)* 2nd ed. (Pergamon, Oxford, 1982).

[34] E. Forest and R. D. Ruth, Physica D **43**, 105 (1990).

[35] J. Candy and W. Rozmus, J. Comp. Phys. **92**, 230 (1991).

[36] J. Javanainen, J. H. Eberly, and Q. Su, Phys. Rev. A **38**, 3430 (1988).

[37] S. C. Rae, X. Chen, and K. Burnett, Phys. Rev. A **50**, 1946 (1994).

[38] W. Becker, X. J. Liu, P. J. Ho, and J. H. Eberly, Rev. Mod. Phys. **84**, 1011 (2012).

[39] C. Jung and H. J. Scholz, J. Phys. A **20**, 3607 (1987).

[40] C. Jung and H. J. Scholz, J. Phys. A **21**, 2301 (1988).

[41] E. Ott and T. Tél, Chaos **3**, 417 (1993).

[42] I. Ya. Berson, Zh. Eksp. Teor. Fiz. **80**, 1727 (1981) [Sov. Phys. JETP **53**, 891 (1982)]

[43] R. V. Jensen, Phys. Rev. A **30**, 386 (1984).

[44] J. G. Leopold and D. Richards, J. Phys. B: At. Mol. Phys. **18**, 3369 (1985).

[45] I. Ya. Berson, Phys. Lett. A **84A**, 364 (1981).

[46] M. S. Child, in *Dynamics of Molecular Collisions*, ed. W. H. Miller, (Springer Science+Business Media, New York, 1976), p. 171.

[47] C. Lanczos, *The variational principles of mechanics*, (University of Toronto Press, Toronto, 1952)

[48] V. Szebehely, *Theory of orbits : The restricted problem of three bodies* (Academic Press, 1967)

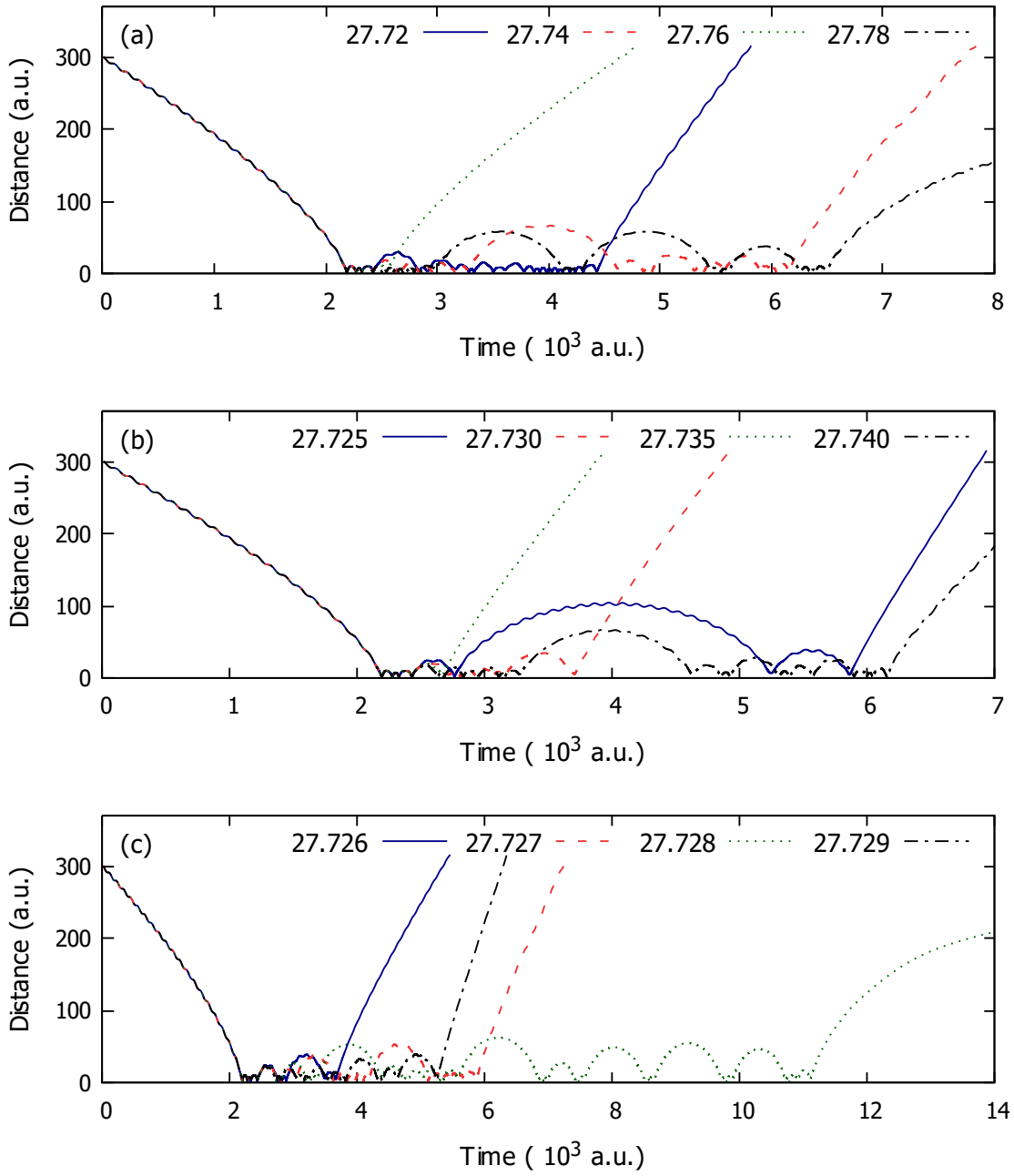

FIG. 11: Electron distance from the Coulomb center as a function of time for several impact parameters b given at the top of each panel (in a.u.). The field parameters are the same as in Fig. 9. Panels (a)-(c) shows the fractal structure as the step in b decreases.

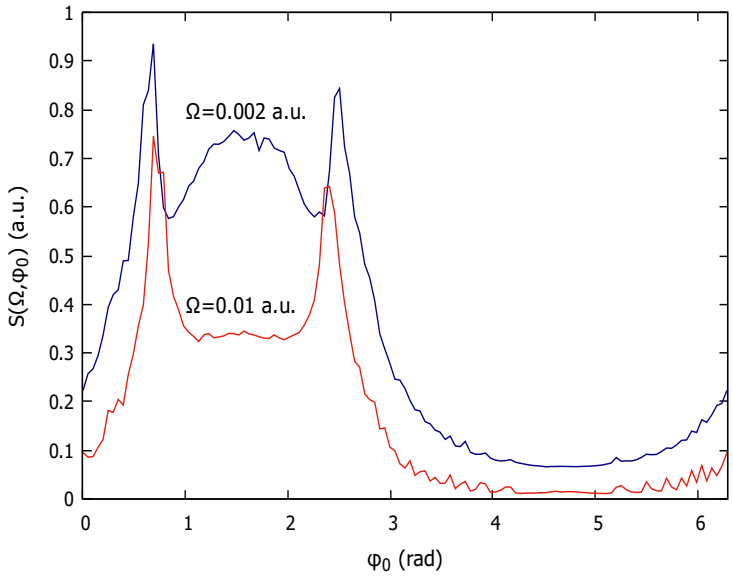

FIG. 12: The bremsstrahlung cross section $S(\Omega, \varphi_0)$ for $F_0 = 0.0056$, $\omega = 0.05696$ a.u., $\Omega = 0.002$ and 0.01 a.u. as a function of the phase φ_0.

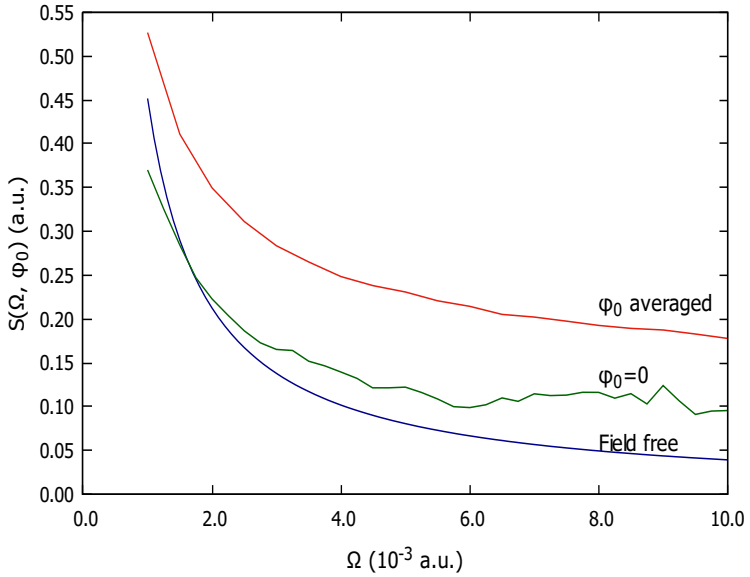

FIG. 13: The bremsstrahlung cross section $S(\Omega, \varphi_0)$ for radiation of infrared photons in the range $\lambda = 4.56$ to 22.8 μm.The field parameters are $F_0 = 0.0056$ a.u. $\omega = 0.05696$ a.u ($\lambda = 0.8$ μm.) Field-free cross section is compared to the case $\varphi_0 = 0$ and φ_0-averaged cross section.

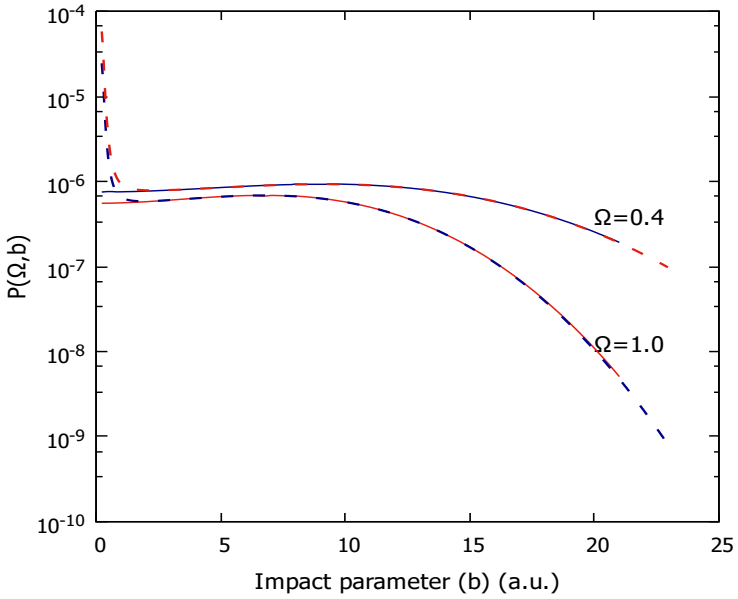

FIG. 14: Probability of spontaneous emission per unit frequency as a function of the impact parameter for the pure Coulomb case, $Z = 1$, $v = 0.1$ a.u. for frequencies $\Omega = 0.4$ and 1.0 a.u. Solid curves: the exact result. The dashed curves diverging near $b = 0$ do not include the velocity correction, Eq. (C1).